Visualizing the connection between edge states and the mobility edge in adiabatic and nonadiabatic topological charge transport

Lizunova, M.A.; Schreck, F.; Morais Smith, C.; Van Wezel, J.

DOI
10.1103/PhysRevB.99.115114

Publication date
2019

Document Version
Final published version

Published in
Physical Review B

Visualizing the connection between edge states and the mobility edge in adiabatic and nonadiabatic topological charge transport

Mariya A. Lizunova,[1,2] Florian Schreck,[3] Cristiane Morais Smith,[1] and Jasper van Wezel[2,*]
[1]*Institute for Theoretical Physics, Utrecht University, Princetonplein 5, 3584 CC Utrecht, The Netherlands*
[2]*Institute for Theoretical Physics Amsterdam, University of Amsterdam, Science Park 904, 1098 XH Amsterdam, The Netherlands*
[3]*Institute of Physics, University of Amsterdam, Science Park 904, 1098 XH Amsterdam, The Netherlands*

(Received 15 November 2018; revised manuscript received 26 February 2019; published 11 March 2019)

The ability to pump quantized amounts of charge is one of the hallmarks of topological materials. An archetypical example is Laughlin's gauge argument for transporting an integer number of electrons between the edges of a quantum Hall cylinder upon insertion of a magnetic flux quantum. This is mathematically equivalent to the equally famous suggestion of Thouless that an integer number of electrons is pumped between two ends of a one-dimensional quantum wire upon sliding a charge-density wave over a single wavelength. We use the correspondence between these descriptions to visualize the detailed dynamics of the electron flow during a single pumping cycle, which is difficult to do directly in the quantum Hall setup because of the gauge freedom inherent in its description. We find a close correspondence between topological edge states and the mobility edges in charge-density wave, quantum Hall, and other topological systems. We illustrate this connection by describing an alternative, nonadiabatic mode of topological transport that displaces precisely the opposite amount of charge compared to the adiabatic pump. We discuss possible experimental realizations in the context of ultracold atoms and photonic waveguide experiments.

DOI: 10.1103/PhysRevB.99.115114

I. INTRODUCTION

The experimental discovery of the integer quantum Hall effect (IQHE) in GaAs [1] revealed the first example of a two-dimensional (2D) material that has an insulating bulk but metallic edge states. The IQHE state is now understood to be part of a much larger class of topological insulators [2–9], which can be labeled by topological invariants such as the Chern number or spin-Chern number [10]. Although these indices determine the number and types of states localized on the edges of a finite sample, they may be computed entirely from bulk quantities and depend on the symmetries of the bulk Hamiltonians. Different topological classes emerge depending on whether time-reversal, particle-hole, and chiral symmetries are present or not [11,12] and may be further refined using lattice symmetries [13–17].

A correspondence between the bulk topological invariants and the dynamics of edge states in the IQHE was put forward by Laughlin [10,18–20]. It shows that adiabatically threading a single Aharonov-Bohm flux quantum $\phi_0 = h/e$ through the interior of an IQHE cylinder [18,19] results in a quantized number of electrons moving from one edge of the cylinder to the opposite. The amount of charge transported is given precisely by the bulk Chern number, defined as an integral over the 2D Brillouin zone [21]. The resulting cyclic charge transfer may be regarded as a dynamical manifestation of the IQHE [22] and has been observed in a Corbino geometry [23,24]. More generally, it is an example of the type of quantized adiabatic particle transport or topological charge pumping first proposed by Thouless [10,21,25,26]. Experimentally, topological pumps have been realized in cold-atom [27,28] and single-spin [29] systems and have attracted attention in both the adiabatic [30,31] and nonadiabatic [32,33] regimes.

Despite its status as an archetype of topological transport, the detailed dynamics of exactly how electrons are transferred between edges as a quantum of flux is threaded through Laughlin's IQHE cylinder remains difficult to visualize. The straightforward comparison of electronic wave functions for values of the flux that differ by fractions of the flux quantum is hampered by the flux dependence of the canonical momentum. In this paper, we circumvent this problem by using a well-known family of one-dimensional (1D) charge-ordered systems that can be mathematically mapped onto the 2D IQHE setup [34]. This allows us to directly visualize the topological transport in real space and time, as electrons flow from one edge of the system to the other, and thus to clarify the nature of the transport in both the charge-ordered and IQHE systems.

The rendering of edge state dynamics additionally reveals the in-gap states are connected to the so-called mobility edge, which is the critical state separating extended from localized states in the bulk of a disordered system [35,36]. In the case of quantum Hall systems, the bulk extended states are known to be constricted to just a single energy in the center of each (impurity-broadened) Landau level, as long as inter-Landau-level scattering is negligible [35,37]. Both edge states and the mobility edge are topological in nature [38], which we confirm by considering their common insensitivity to the presence of weak impurities. Together, the edge states and the mobility edges make up a single set of connected states winding around the electronic spectrum. We illustrate

*vanwezel@uva.nl

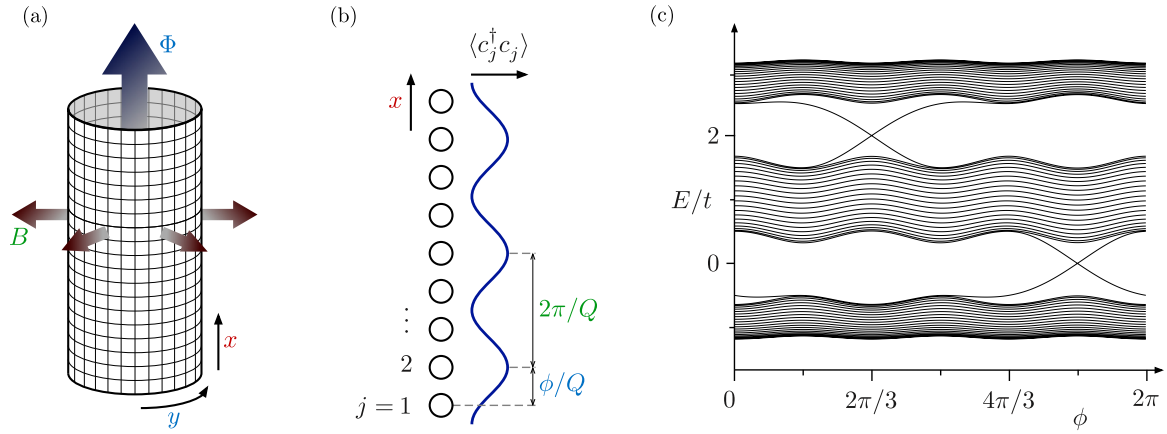

FIG. 1. Schematic depictions of (a) the quantum Hall cylinder used in Laughlin's gauge argument and (b) the mean-field charge-density wave (CDW) used as a Thouless pump. Both systems are described by Harper's equation, where the x coordinate is a spatial direction in both cases. The perpendicular magnetic field B in the cylinder plays the same role as the band filling n or, equivalently, propagation vector Q in the CDW. The phase of the charge-density modulation can be mapped to a gauge-independent combination of the y component of momentum and the magnetic flux Φ piercing the quantum hall cylinder. (c) The spectrum of the two systems is the same, including the presence of localized, in-gap modes at the edges of the x direction. Notice that for the CDW, each value of ϕ represents a separate 1D system, while for the 2D quantum Hall cylinder ϕ corresponds to the y component of momentum and states for all values of k_y are simultaneously occupied.

this connection of all the topological states by suggesting an alternative form of topological charge transport based on a nonadiabatic variation of externally applied fields. The nonadiabatic charge pump transfers precisely the opposite amount of charge from its traditional adiabatic counterpart and thus acts as an "anti-Thouless" pump. We suggest a possible experimental realization in cold atomic gases in an optical lattice.

II. MAPPING BETWEEN ONE AND TWO DIMENSIONS

Harper's equation, and, more generally, a Mathieu equation [39–41], can be interpreted both as a tight-binding model for the IQHE in two dimensions and as a family of mean-field descriptions for monatomic commensurate charge-density waves (CDWs) in one dimension [34,42–45]. The filling of the charge-ordered system, and hence its CDW periodicity, for example, can be taken to correspond to the magnetic field strength perpendicular to the surface of a quantum Hall cylinder, which determines the filling of its Landau levels [34,41,43]. Under the same mapping, the phase ϕ of the CDW order parameter then corresponds to a flux threading the quantum Hall cylinder [18], while the spatial coordinate of the CDW chain is directly related to the spatial coordinate parallel to the axis of the 2D cylinder. The mapping is indicated schematically in Fig. 1.

Upon varying the parameter ϕ adiabatically from zero to 2π, the CDW slides along the 1D chain over precisely one wavelength. The flux threading the IQHE system is increased by one quantum under the same variation. When introducing edges, we thus expect to find adiabatic transport of a quantized number of electrons from one side of the system to the other in both cases. In this way, the mapping relates the quantized adiabatic particle transport (Thouless pumping [21]) in charge-ordered systems to the topological transport between edge states upon insertion of a flux quantum in a quantum Hall cylinder (Laughlin's gauge argument [18]).

The bulk of both the CDW and IQHE systems is insulating, and only the edge states cross the Fermi level. By solving Harper's equation on a cylinder, the spectrum can be plotted as a function of momentum in the periodic direction. It consists of bulk bands and isolated topological edge states crossing the gaps between them. The edge states are protected in the sense that the number of edge channels cannot be modified as long as the bulk of the system remains gapped [18]. In a CDW system the periodic direction is given by the mean-field value of the phase variable ϕ, as shown in Fig. 1. Each value of the phase then corresponds to a single realization of a CDW on the chain, which may or may not host edge states. The combined spectrum of the family of CDWs containing all values of ϕ coincides with that of the IQHE cylinder.

To be concrete, consider a CDW on a finite chain of N sites described by the Hamiltonian:

$$H = -t\sum_{j=1}^{N-1}(c_j^\dagger c_{j+1} + c_{j+1}^\dagger c_j) + V\sum_{j=1}^{N-1} c_j^\dagger c_j c_{j+1}^\dagger c_{j+1} + \sum_{j=1}^{N}\zeta_j\, c_j^\dagger c_j. \quad (1)$$

Here, $t > 0$ is the tunneling amplitude, V is the strength of the nearest-neighbor Coulomb interaction between electrons, and ζ_j is a random on-site potential that describes the effect of impurities. The operator $c_j^\dagger$ (c_j) creates (annihilates) a spinless electron at position $x = ja$, where a is the lattice constant. The filling factor n is a common fraction, so that Nn is the total number of electrons in the system. As usual, we assume the system is charge neutral in total and ignore any ionic charges.

Using the mean-field ansatz $\langle c_{j+1}^\dagger c_{j+1} + c_{j-1}^\dagger c_{j-1}\rangle \approx 2\langle c_j^\dagger c_j\rangle = A\cos(Qja+\phi)$ for the particle density, the interaction term becomes $\sum_j VA\cos(Qja+\phi)c_j^\dagger c_j$ [34]. This ansatz defines the propagation vector $Q = 2\pi n/a$ of the charge-density modulations, as well as the phase ϕ, which

determines the position of the CDW with respect to the lattice. Substituting the interaction back into Eq. (1) yields the full mean-field Hamiltonian for the 1D CDW chain. For periodic boundary conditions and $\zeta_j = 0$, this form of the Hamiltonian will coincide with Hofstadter's tight-binding description of the IQHE [41] if we make the identifications $k \to k_x$, $Q \to eB/(\hbar c)$ and $\phi \to k_y a$. Here, k is the momentum in the CDW, and $k_{x,y}$ are the x, y components of momentum in the IQHE. The radial magnetic field B in the IQHE cylinder determines the filling of its Landau levels. Under this mapping, adding flux along the central axis of the IQHE cylinder corresponds to changing the value of the phase ϕ in the CDW [18] and thus to sliding the charge-density wave along the chain.

The Hamiltonian itself may be realized as a mean-field description of charge order in 1D chains of aligned orbitals within a three-dimensional material [46] or as an effective description of cold atoms in an optical lattice [34,47]. Here, we focus first on the topological properties of the theoretical mean-field model, before discussing possible experimental probes of the various emerging modes of topological transport in more realistic settings.

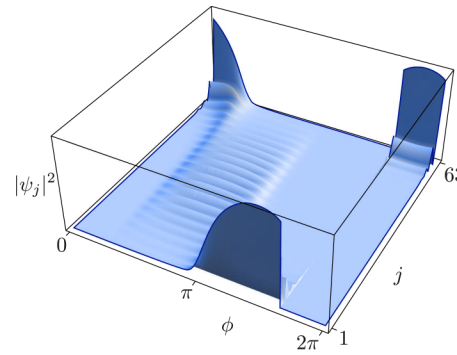

FIG. 2. The squared amplitude of the highest occupied wave function at 1/3 filling as a function of phase ϕ and position j along the CDW chain. The bulk state between $\phi \approx \pi/3$ and $\phi \approx \pi$ can be recognized as a particle in a box eigenfunction with additional CDW modulations. It undergoes an avoided crossing at $\phi \approx \pi$ and becomes a left edge state for values of ϕ up to $5\pi/3$, where it changes abruptly into a right edge state until coming back to $\phi \approx \pi/3$. If opposing edges of the chain are connected, the abrupt tunneling from left to right will turn into an avoided crossing of its own, whose adiabatic traversal may correspond, for example, to the physical process of charge being transferred from one edge to another through an intermediary wire.

III. VISUALIZING CHARGE TRANSFER BETWEEN EDGE STATES

In Laughlin's argument for quantized transport across the IQHE cylinder [18], the electromagnetic gauge structure plays a central role. Although helpful in establishing why the charge transferred between the ends of the cylinder must be an integer, the presence of gauge freedom makes it hard to directly visualize the precise dynamics. We know and understand what happens upon insertion of a single flux quantum, but questions like at which value of the flux one edge state becomes unoccupied and the opposite one becomes occupied and what the wave function looks like after insertion of only half a flux quantum are difficult to answer in a gauge-independent fashion. For the CDW system, this problem does not exist. The process corresponding to a flux insertion is the sliding of the CDW by precisely one wavelength, and this results in a precisely quantized amount of charge being transferred from one end of the chain to the other (Thouless pumping [21]). The quantized conductivity is determined by the sum of Chern numbers for all occupied bands (in k, ϕ space), as in the IQHE. However, in this case we can plot the charge distribution for both bulk and edge states for any value of ϕ and hence visualize the topological transport as a continuous process.

As shown in Fig. 1, the spectrum and eigenstates can be computed for a specific choice of parameter values, including any value for the phase ϕ. As an example, we show the results for a period-3 CDW with $n = 1/3, N = 63$, and $AV/t = 5$. We use this specific example throughout the paper but note that taking other parameter choices does not qualitatively affect any of our results. Among the numerically obtained wave functions, bulk and edge states can easily be distinguished. The bulk wave functions for a CDW with open boundary conditions can be understood as products of plane waves (solutions of a CDW system with periodic boundary conditions) and the eigenstates of a particle in a box. The edge states, on the other hand, are exponentially localized on one side of the chain.

Upon varying ϕ, the highest occupied state changes from an edge state localized on one side to that on the opposite side. In the example of 1/3 filling shown in Fig. 2, the highest state with $E < 0$ at $\phi = 0$ is an edge state localized on the right side of the chain ($j = 63$). In the region $\pi/3 \lesssim \phi \lesssim \pi$, the edge state is adiabatically transformed into a bulk state, until it emerges again as an edge state on the opposite side of the system. At $\phi \simeq 5\pi/3$, the highest occupied state discontinuously changes from being localized on the left side of the chain ($j = 1$) to being localized on the right. From the spectrum, it is clear that this behavior stems from the two edge states crossing in energy at this point.

Notice that the states displayed in Fig. 2 are the highest occupied states at zero temperature for a given value of the phase variable ϕ. Starting from a phase value $\phi < 5\pi/3$ and adiabatically sliding the CDW forward, the system will, in fact, not stay in the instantaneous ground state. The two edge states crossing within the bulk gap are located at opposite edges of the chain in real space, and any matrix element of local operators that could assist in tunneling across is exponentially small in the chain length. A state on one end of the system can therefore not simply jump to the other end in the way suggested by Fig. 2. For a sufficiently long CDW, adiabatic variation of ϕ causes the system to end up in an excited state at $\phi = 2\pi$, with a high-energy edge state occupied and a lower-energy edge state empty. The system can only return to its instantaneous ground state, and the topological material can only function as an adiabatic charge pump if the two edges of the CDW chain are connected to one another through some external coupling. In fact, in any experimental implementation of a topological quantum pump, one would indeed include a wire connecting the two sides of

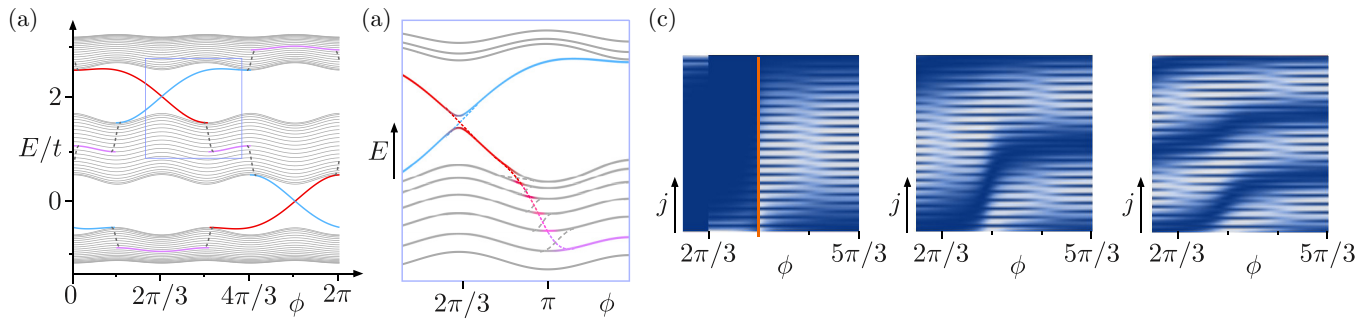

FIG. 3. (a) Sketch of the spectrum as a function of the phase ϕ with all states related to the topological order indicated. Red lines crossing bulk gaps are edge states localized at the left ($j = 1$) end of the chain, blue lines are right ($j = 63$) edge states, and purple lines in the middle of bulk bands represent mobility edges. (b) Schematic close-up view of the crossing of two edge states and of an edge state entering the bulk band. If the two edges are connected, they undergo an avoided crossing, which can be traversed either adiabatically by tuning ϕ very slowly or nonadiabatically by increasing ϕ more rapidly in the region of the avoided crossing. As the edge state enters the bulk band, it necessarily undergoes a series of avoided crossings, which ultimately connect the edge state to the mobility edge. (c) Intensity plot of selected wave function amplitudes $|\psi_j(\phi)|^2$ for different values of the phase ϕ. In all plots, dark blue and white indicate low and high amplitudes, respectively. The leftmost plot shows the state which in (b) starts out as a right edge state (blue line) for low ϕ, then becomes a left edge state (red line), and after the avoided crossing at $\phi \simeq \pi$ becomes a bulk state (gray line). The orange line in (c) indicates that separate color scales were used for the edge and bulk states. The other two panels show the states that start out at low ϕ as the topmost state in the lower bulk band and the one below it. The avoided crossings at $\phi \simeq \pi$ can be identified by the changing number of nodes in the wave function.

the system and would typically measure the current through the wire as the phase is being varied. Such a connection can easily be included in the simulation as a weak hopping element between the opposing sides of the chain. It allows the two edge states to interact and turns their intersection in the spectrum into an avoided crossing by opening up a small energy gap. Adiabatic evolution, which retains the instantaneous ground state throughout a pumping cycle, is once again possible. Varying ϕ from zero to 2π then results in the transfer of precisely one (the Chern number of the lowest band in k, ϕ space [34]) electron from one side of the system to the other, through the connecting wire, and thus realizes the Thouless pump or, in the IQHE interpretation of the same system, Laughlin's gauge argument.

IV. THE CONNECTION OF EDGE STATES TO THE MOBILITY EDGE

Inspecting the bulk wave functions in the spectrum of Fig. 1, two features stand out. First of all, as the edge state enters the bulk band, it does not simply disappear. Tracking, for example, the highest occupied state in Fig. 1, it is clear that the state, which was an edge state at $\phi < \pi/3$, becomes a bulk state at $\pi/3 \lesssim \phi \lesssim \pi$. The bulk state is the particle in a box state with the highest available number of nodes, dressed with charge-density modulations. A state with the same number of nodes in fact already existed for $\phi < \pi/3$ as part of the occupied bulk states. The edge state therefore does not evolve into a new bulk state as ϕ is adiabatically changed, but rather has an avoided crossing with an existing bulk state and takes over its character. The existing bulk state takes over the character of the edge state and is pushed down in energy in the process. It then has an avoided crossing with the next bulk state and so on. This pattern is shown schematically in Fig. 3.

Close inspection of the wave functions in the spectrum indeed shows a cascade of avoided crossings, witnessed by the remainder of an exponential localization that is visible in bulk states undergoing the avoided crossings. These continue until the edge state reaches precisely the middle of the bulk band. There, it emerges again for an extended range of ϕ in the form of another well-known topologically special state, the mobility edge [35]. This isolated critical state was to be expected in the center of the bulk band because the extended bulk states generic to the disordered system are known to be constricted to just a single energy precisely in the center of each (impurity-broadened) Landau level in the case of the quantum Hall effect [37]. Just like the mobility edge was formed from a left edge state at $\phi \simeq \pi/3$, it goes through a second series of avoided crossing and reemerges as a right edge state at $\phi \simeq \pi$. The edge states are of the form $\psi(x) \propto e^{\lambda x}$, with λ being negative and positive for edge states localized at small and large x, respectively. The mobility edge naturally connects these two states and has the same shape of the wave function, with $\lambda = 0$. This special, totally delocalized wave function is thus a plane wave connecting both sides of the sample. Within the CDW, the plane wave is again dressed by charge modulations, as shown in Fig. 4. Note that for even Nn, it is possible to have two orthogonal, delocalized wave functions. We consider chains with odd Nn here, so that a single mobility edge connects to edge states in both bulk gaps.

The topological nature of the mobility edge becomes apparent upon adding a random impurity potential ζ_j. Notice that in contrast to the IQHE, where the presence of weak impurities is necessary to observe the quantization of the Hall conductivity, in the CDW system topological transport may be observed even with only the Coulomb interaction localizing charges within the unit cell. Nevertheless, the presence of weak impurities (modeled here with $|\zeta_j|/t < 0.2$) may be considered, and their effect is much the same as in the IQHE, localizing electronic states at specific locations in the chain. The difference between the mobility edge and other bulk states is now immediately obvious. As shown in Fig. 4, typical

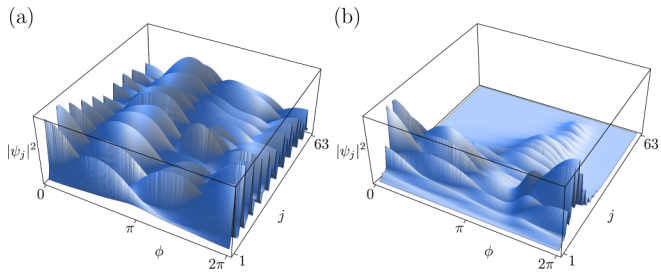

FIG. 4. Wave functions in the presence of randomly distributed weak impurities ($|\zeta_j|/t < 0.2$). The delocalized mobility edge in (a) is hardly affected by the impurities, testifying to its topological character. The lowest-energy state in (b), on the other hand, becomes completely localized at the location of the strongest impurity. For both panels, the same distribution of impurities was used.

bulk states are severely affected by the impurity potential, being amplified and suppressed at random locations. The mobility edge, on the other hand, retains a more or less constant amplitude along the entire length of the chain, as long as the impurity strength is weak. This clearly indicates the topological nature of the mobility edge and hence its connection with the topological edge states.

V. NONADIABATIC QUANTIZED PARTICLE TRANSPORT

The connection between edge states and the mobility edge may be illustrated by considering a nonadiabatic mode of quantized transport, which exists in addition to the well-known adiabatic Thouless pump. Starting, for example, with the (red) left edge state just below $\phi \simeq 5\pi/3$ being occupied, an induced nonadiabatic evolution that jumps all avoided crossings with both bulk and edge states would result in the highest occupied state going around the full spectrum, as shown schematically in Fig. 3. As ϕ is increased by 6π, the highest occupied state traverses all topologically special states in the entire spectrum and returns to its initial configuration. When stopping the nonadiabatic evolution after ϕ is increased by 4π, however, the highest occupied state will have moved from its initial left edge state to the right edge state in the lowest bulk gap. In the presence of a wire connecting both ends of the chain, we can then either adiabatically increase ϕ by another $2\pi/3$ or let the system spontaneously relax to its ground state. Both will lead to the excited state going from right to left through the wire. That is, a current is carried through the connecting wire in the direction opposite to that of the usual adiabatic topological transport. This nonadiabatic transfer of charge with the same magnitude but in the opposite direction of the usual Thouless pumping is made possible by the edge states and mobility edges forming a connected set of states winding throughout the electronic spectrum.

Generalizing the procedure to systems of any filling, the integer number of charges transferred by the nonadiabatic mode of transport will equal $-C$, with C being the total Chern number of all occupied bands, the exact opposite of the C electrons conveyed in the usual Thouless pump. In this sense, it acts as a sort of anti-Thouless pump. Notice that hybrid protocols employing both adiabatic and nonadiabatic driving can accomplish the same thing in a much simpler fashion. In such protocols, however, the highest occupied state is in nontopological, localized bulk states for part of the pumping cycle. The purely nonadiabatic process suggested here, in which the highest occupied state jumps all avoided crossings that it encounters, is special because it depends entirely on the special nature and connectivity of the topological edge states and mobility edge states.

The nonadiabatic topological charge pump presented here is intended purely as an illustration of the connection between different types of topological states. Nevertheless, nonadiabatic or hybrid protocols may in some aspects be preferable to purely adiabatic ones in practical implementations of topological pumping. As was recently pointed out, the presence of a spectrum of unoccupied states imposes much more stringent conditions for achieving adiabaticity than just the timescale of the driving being longer than the inverse gap size [48–50]. Nonadiabatic driving across an avoided crossing, on the other hand, can be accomplished by sufficiently fast changes in the driving parameters, as long as the overlap between initial and target states is large. We confirmed that this is the case in the model CDW system by achieving an almost complete transfer of occupation across avoided crossings upon ramping up the driving speed. For any experimental implementation, a practical restriction on parameter values may arise from a preference for maintaining the validity of the mean-field solution even under nonadiabatic driving.

VI. A POSSIBLE IMPLEMENTATION

To realize the proposed illustration of a nonadiabatic pumping cycle in experiments, several techniques for imaging the real-space structure of CDW systems can be used. First of all, the static real-space structure of a CDW can be imaged by scanning tunneling microscopy (STM), which directly observes the amplitude and phase of charge-density modulations induced by a CDW [51–54], as well as excess charge at the end of a chain [55]. Straightforward experimental realizations of the dynamic quantized transport protocols, on the other hand, may use ultracold atoms in an optical lattice or photons in a waveguide array. Waveguide arrays may directly simulate the CDW Hamiltonian [55]. Variations of the mean-field CDW phase ϕ are then implemented by appropriate variations of the index of refraction. The quantized transport of charge can be observed by injecting photons into the waveguide at one edge and observing the intensity distribution in the waveguides after various propagation distances. The required values for experimental parameters are similar to those used in the literature [55] and can be realistically obtained with existing technology.

Using ultracold atoms, the mean-field Hamiltonian can be constructed by projecting a circular optical dipole lattice of 63 sites through a microscope objective [47,56]. This can be done, for example, using an objective with a numerical aperture of 0.8 [57] and a short wavelength of 532 nm [58], obtaining a waist of the projected Gaussian beams of the order of 0.4 μm. To ensure that the projected potential is attractive at this wavelength, one could use, for example, Sr atoms to load the lattice. Gaussian beams with a spacing of 0.7 μm then result in a potential that closely resembles a sine wave. The lattice depth will be approximately 0.3 times the depth

of one Gaussian beam. The lattice sites can be created by imaging a mask or a pattern from a digital mirror device (DMD) through the objective [47]. In order to confine the atoms in the direction orthogonal to the plane of the ring, an optical lattice can be applied in that direction.

Appropriate values of the model parameters, establishing a Mott-insulator regime with a weak residual tunneling, may be achieved, for example, by choosing a lattice depth of about eight recoil energies, or approximately 10 kHz. The mean-field energies are then $V = 270$ Hz and $t = 45$ Hz. A weak link may be introduced between two particular sites in the lattice to allow them to act as edges. The strength of the tunneling across the weak link can be adjusted arbitrarily far down from 45 Hz by increasing the spacing between the two selected sites.

To create and move the CDW, an additional lattice with larger spacing may be added [28]. The required specifics for this additional lattice are much more relaxed than the ones for the primary lattice and can be freely adjusted within a sizable range. The rotation of the secondary lattice could be achieved by imaging a DMD or a rotating mask onto the atoms. The lifetime of the system is limited by off-resonant scattering of the strongest, primary lattice, which for the parameters discussed above will be over 200 s. The experiment should take a few times 63 tunnel times, which is a few times 2.8 s, and therefore comfortably fits in the expected experimental lifetime. The system can be prepared in its ground state by using the Mott-insulator transition. After a full driving cycle, the quantized buildup of charge at the edges can be detected by quantum gas microscopy, which directly measures the parity of the number of atoms in each lattice well. All of this can be realistically done with existing technology.

VII. CONCLUSIONS

We propose a procedure to visualize adiabatic and nonadiabatic topological charge transport in a 1D charge-ordered system, which is well known to map precisely onto the tight-binding model for the 2D IQHE in the Landau gauge used by Laughlin to explain topological transport in an IQHE cylinder. The absence of an electromagnetic field in the CDW, and hence of the need to make a gauge choice, enables us to directly compare plots of wave functions at different values of the CDW phase. The topological transport and dynamics of electrons in the CDW chain found here thus give direct insight into the detailed motion of electronic states in the IQHE as well.

The visualization of the topological transport brings to the fore an explicit connection between edge states localized at the ends of the chain or cylinder and the mobility edges residing in the very center of their bulk states. To illustrate the connection between these two types of topological states, localized and extended, we formulate a purely nonadiabatic protocol that nonetheless results in quantized, topological transport of charge. The number of electrons pumped in a single cycle is precisely equal to that of the well-known adiabatic pump, but they flow in the opposite direction, creating a sort of anti-Thouless pump. We expect our conclusions, in particular the connection between edge states and the bulk mobility edge, to apply more generally to disordered topological systems. Any system with a nontrivial Chern or Z_2 invariant is guaranteed to have edge states, and similarly, mobility edges arise generically in models with disorder-induced localization. A simplified intuitive picture of the connection between the two types of states, suggested by the CDW system studied here, can then be drawn starting from an edge state localized on one side of the system. By evolving this state as a function of some system parameter, such as the CDW phase, it may be adiabatically connected to an edge state on the opposite side of the system. If the evolution is adiabatic throughout, however, a fully delocalized state must generically exist between the two edge-localized extremes.

Finally, we suggest experiments on ultracold atoms in an optical lattice, as well as in photonic waveguides, which can test the proposed connection between edge states and mobility edges, as well as the nonadiabatic pumping cycle, using realistic parameter values.

ACKNOWLEDGMENTS

This work is part of the Delta Institute for Theoretical Physics (DITP) consortium, a program of the Netherlands Organization for Scientific Research (NWO) that is funded by the Dutch Ministry of Education, Culture and Science (OCW). J.v.W. acknowledges support from a VIDI grant financed by NWO. This project has received funding from the European Research Council (ERC) under the European Union's Seventh Framework Programme (FP7/2007-2013; Grant Agreement No. 615117 QuantStro).

[1] K. von Klitzing, G. Dorda, and M. Pepper, Phys. Rev. Lett. **45**, 494 (1980).
[2] B. A. Bernevig, T. L. Hughes, and S.-C. Zhang, Science **314**, 1757 (2006).
[3] M. Koenig, S. Wiedmann, C. Bruene, A. Roth, H. Buhmann, L. W. Molenkamp, X.-L. Qi, and S.-C. Zhang, Science **318**, 766 (2007).
[4] C. L. Kane and E. J. Mele, Phys. Rev. Lett. **95**, 226801 (2005).
[5] C. L. Kane and E. J. Mele, Phys. Rev. Lett. **95**, 146802 (2005).
[6] X.-L. Qi and S.-C. Zhang, Phys. Today **63**(1), 33 (2010).
[7] M. Z. Hasan and C. L. Kane, Rev. Mod. Phys. **82**, 3045 (2010).
[8] X.-L. Qi and S.-C. Zhang, Rev. Mod. Phys. **83**, 1057 (2011).
[9] R.-J. Slager, A. Mesaros, V. Juričić, and J. Zaanen, Nat. Phys. **9**, 98 (2013).
[10] D. J. Thouless, M. Kohmoto, M. P. Nightingale, and M. den Nijs, Phys. Rev. Lett. **49**, 405 (1982).
[11] A. Altland and M. R. Zirnbauer, Phys. Rev. B **55**, 1142 (1997).
[12] S. Ryu, A. Schnyder, A. Furusaki, and A. Ludwig, New J. Phys. **12**, 065010 (2010).
[13] J. Kruthoff, J. de Boer, J. van Wezel, C. L. Kane, and R.-J. Slager, Phys. Rev. X **7**, 041069 (2017).
[14] J. Kruthoff, J. de Boer, and J. van Wezel, arXiv:1711.04769.

[15] H. C. Po, A. Vishwanath, and H. Watanabe, Nat. Commun. **8**, 50 (2017).
[16] H. Watanabe, H. C. Po, and A. Vishwanath, Sci. Adv. **4**, eaat8685 (2018).
[17] B. Bradlyn, L. Elcoro, J. Cano, M. G. Vergniory, Z. Wang, C. Felser, M. I. Aroyo, and B. A. Bernevig, Nature (London) **547**, 298 (2017).
[18] R. B. Laughlin, Phys. Rev. B **23**, 5632 (1981).
[19] B. I. Halperin, Phys. Rev. B **25**, 2185 (1982).
[20] Y. Hatsugai, Phys. Rev. Lett. **71**, 3697 (1993).
[21] D. J. Thouless, Phys. Rev. B **27**, 6083 (1983).
[22] V. Gritsev and A. Polkovnikov, Proc. Natl. Acad. Sci. U.S.A. **109**, 6457 (2012).
[23] V. T. Dolgopolov, A. A. Shashkin, N. B. Zhitenev, S. I. Dorozhkin, and K. von Klitzing, Phys. Rev. B **46**, 12560 (1992).
[24] A. B. Vorob'ev, V. Y. Prinz, Y. S. Yukecheva, and A. I. Toropov, Phys. E (Amsterdam, Neth.) **23**, 171 (2004).
[25] Q. Niu, Phys. Rev. B **34**, 5093 (1986).
[26] D. Xiao, M.-C. Chang, and Q. Niu, Rev. Mod. Phys. **82**, 1959 (2010).
[27] S. Nakajima, T. Tomita, S. Taie, T. Ichinose, H. Ozawa, L. Wang, M. Troyer, and Y. Takahashi, Nat. Phys. **12**, 296 (2016).
[28] M. Lohse, C. Schweizer, O. Zilberberg, M. Aidelsburger, and I. Bloch, Nat. Phys. **12**, 350 (2016).
[29] W. Ma, L. Zhou, Q. Zhang, M. Li, C. Cheng, J. Geng, X. Rong, F. Shi, J. Gong, and J. Du, Phys. Rev. Lett. **120**, 120501 (2018).
[30] B. L. Altshuler and L. I. Glazman, Science **283**, 1864 (1999).
[31] M. Switkes, C. M. Marcus, K. Campman, and A. C. Gossard, Science **283**, 1905 (1999).
[32] M. Moskalets and M. Buttiker, Phys. Rev. B **66**, 205320 (2002).
[33] I. Maruyama and Y. Hatsugai, J. Phys.: Conf. Ser. **150**, 022055 (2009).
[34] F. Flicker and J. van Wezel, Europhys. Lett. **111**, 37008 (2015).
[35] B. Huckestein, Rev. Mod. Phys. **67**, 357 (1995).
[36] D. M. Basko, I. L. Aleiner, and B. L. Altshuler, Ann. Phys. (NY) **321**, 1126 (2006).
[37] J. T. Chalker, J. Phys. C **20**, L493 (1987).
[38] A. M. M. Pruisken, Int. J. Mod. Phys. B **24**, 1895 (2010).
[39] P. G. Harper, Proc. Phys. Soc. London, Ser. A **68**, 874 (1955).
[40] J. Bellissard and B. Simon, J. Funct. Anal. **48**, 408 (1982).
[41] D. R. Hofstadter, Phys. Rev. B **14**, 2239 (1976).
[42] R. Peierls, Ann. Phys. (Leipzig) **396**, 121 (1930).
[43] J. Klinovaja and D. Loss, Phys. Rev. Lett. **111**, 196401 (2013).
[44] J. Klinovaja and D. Loss, Eur. Phys. J. B **87**, 171 (2014).
[45] M. Thakurathi, J. Klinovaja, and D. Loss, Phys. Rev. B **98**, 245404 (2018).
[46] G. Grüner, Rev. Mod. Phys. **60**, 1129 (1988).
[47] L.-C. Ha, L. W. Clark, C. V. Parker, B. M. Anderson, and C. Chin, Phys. Rev. Lett. **114**, 055301 (2015).
[48] O. Lychkovskiy, O. Gamayun, and V. Cheianov, Phys. Rev. Lett. **119**, 200401 (2017).
[49] O. Lychkovskiy, O. Gamayun, and V. Cheianov, in *Fourth International Conference on Quantum Technologies (ICQT-2017)*, edited by A. I. Lvovsky, M. L. Gorodetsky and A. N. Rubtsov, AIP Conf. Proc. No. 1936 (AIP, New York, 2018), p. 020024.
[50] A. Polkovnikov and V. Gritsev, Nat. Phys. **4**, 477 (2008).
[51] P. C. Snijders, S. Rogge, and H. H. Weitering, Phys. Rev. Lett. **96**, 076801 (2006).
[52] C. Brun, Z.-Z. Wang, P. Monceau, and S. Brazovskii, Phys. Rev. Lett. **104**, 256403 (2010).
[53] A. Soumyanarayanan, M. M. Yee, Y. He, J. van Wezel, D. J. Rahn, K. Rossnagel, E. W. Hudson, M. R. Norman, and J. E. Hoffman, Proc. Natl. Acad. Sci. U.S.A. **110**, 1623 (2013).
[54] M. M. Ugeda, A. J. Bradley, Y. Zhang, S. Onishi, Y. Chen, W. Ruan, C. Ojeda-Aristizabal, H. Ryu, M. T. Edmonds, H.-Z. Tsai, A. Riss, S.-K. Mo, D. Lee, A. Zettl, Z. Hussain, Z.-X. Shen, and M. F. Crommie, Nat. Phys. **12**, 92 (2016).
[55] Y. E. Kraus, Y. Lahini, Z. Ringel, M. Verbin, and O. Zilberberg, Phys. Rev. Lett. **109**, 106402 (2012).
[56] M. Lohse, C. Schweizer, H. M. Price, O. Zilberberg, and I. Bloch, Nature (London) **553**, 55 (2018).
[57] W. S. Bakr, J. I. Gillen, A. Peng, S. Fölling, and M. Greiner, Nature (London) **462**, 74 (2009).
[58] M. A. Norcia, A. W. Young, and A. M. Kaufman, Phys. Rev. X **8**, 041054 (2018).